

Combined Raman and IR study of $\text{MO}_x\text{-V}_2\text{O}_5/\text{Al}_2\text{O}_3$ ($\text{MO}_x = \text{MoO}_3, \text{WO}_3, \text{NiO}, \text{CoO}$) catalysts under dehydrated conditions

Michael A. Vuurman,^a Derk J. Stufkens,^a Ad Oskam,^a Goutam Deo^b and Israel E. Wachs^{b*}

^a Department of Chemical Engineering, University of Amsterdam, Nieuwe Achtergracht 166, 1018WV, Amsterdam, The Netherlands

^b Zettlemoyer Center for Surface Studies, and Department of Chemical Engineering, Lehigh University, Bethlehem, PA 18015, USA

The influence of a second metal oxide (tungsten oxide, molybdenum oxide, nickel oxide, cobalt oxide) upon a $\text{V}_2\text{O}_5/\text{Al}_2\text{O}_3$ catalyst has been investigated by a combined Raman and IR study under dehydrated conditions. The presence of tungsten or molybdenum oxide was found to increase the concentration of polymerized surface vanadium oxide species, and this reflects the higher surface coverages of the metal oxides on the alumina support. This is probably caused by competition between vanadium and molybdenum oxide (or vanadium and tungsten oxide) species for reaction with the alumina hydroxy groups, since the IR spectra showed that on addition of these metal oxides the same type of alumina hydroxy groups are consumed. The presence of nickel or cobalt oxide on alumina increases the concentration of polymerized vanadium oxide species dramatically, which indicates that the presence of these oxides is also experienced by the surface vanadium oxide. However, the hydroxy groups are not affected as they are for the molybdenum and tungsten oxide systems.

It has been suggested that there are two types of supported metal oxides on $\gamma\text{-Al}_2\text{O}_3$.¹ The first type is metal oxides having a high oxidation state (Re^{7+} , Mo^{6+} , W^{6+} , Cr^{6+} , Nb^{5+} and V^{5+}), and their surface structures are sensitive to the presence of water vapour.² This moisture is adsorbed from the air when the sample is exposed to laboratory atmosphere after calcination. Owing to the presence of the adsorbed moisture, the surface metal oxides are hydrated and their surface structures become similar to those observed in aqueous solution.² Upon heating at elevated temperatures, the adsorbed moisture is desorbed.³ As a consequence the surface metal oxide becomes dehydrated and the metal oxide structures are generally altered. This has been shown by many recent *in situ* Raman studies, which revealed a drastic change of the metal-oxygen vibrations upon dehydration.^{4–20} The sensitivity to the presence of water vapour has been used as an argument that metal oxides with a high oxidation state are adsorbed on the surface of the support.¹ IR spectroscopy has indicated that under dehydrated conditions the interaction between metal oxide and support surface occurs by consumption of the alumina hydroxy groups.^{11,21–23}

The second type of metal oxide supported on alumina consists of oxides with low oxidation states (*e.g.* Ni^{2+} , Co^{2+} and Fe^{3+}). It has been argued that these metal oxides are absorbed into the subsurface of the alumina support, since they can be accommodated in the $\gamma\text{-Al}_2\text{O}_3$ lattice.^{24–35} Based on Raman spectroscopy, it has been proposed that the supported nickel oxide and iron oxide phases are not sensitive to the presence of moisture.^{1,34} To our knowledge, the influence of these metal oxides (Ni^{2+} , Co^{2+} and Fe^{3+}) on the alumina hydroxy groups has not been studied by IR spectroscopy.

The purpose of the present investigation is to study the interaction between the two types of metal oxides with a $\text{V}_2\text{O}_5/\text{Al}_2\text{O}_3$ catalyst by vibrational spectroscopy and reactivity studies. In the present investigation, the interaction between the metal oxides of a $\text{V}_2\text{O}_5/\text{Al}_2\text{O}_3$ catalyst is determined using Raman and IR spectroscopy. In the following paper, the interaction between the metal oxides with a $\text{V}_2\text{O}_5/\text{Al}_2\text{O}_3$ catalyst is studied for the selective catalytic reduction of NO with NH_3 . To study the interaction of the

first type of metal oxide with a $\text{V}_2\text{O}_5/\text{Al}_2\text{O}_3$ catalyst, $\text{WO}_3\text{-V}_2\text{O}_5/\text{Al}_2\text{O}_3$ and $\text{MoO}_3\text{-V}_2\text{O}_5/\text{Al}_2\text{O}_3$ samples are studied. To study the interaction of the second type of metal oxide with a $\text{V}_2\text{O}_5/\text{Al}_2\text{O}_3$ catalyst, $\text{NiO-V}_2\text{O}_5/\text{Al}_2\text{O}_3$ and $\text{CoO-V}_2\text{O}_5/\text{Al}_2\text{O}_3$ samples are studied. A second aspect of the present study is that the dehydrated surface structures of these supported systems are for the first time characterized by a combined Raman and IR investigation. In addition, the interaction of these metal oxide species with the alumina-support hydroxy groups is studied by monitoring the changes in the OH stretching region by IR spectroscopy.

Experimental

Preparation of catalysts

The support used in this study was γ -alumina (Harshaw, 180 $\text{m}^2 \text{g}^{-1}$). The 10% $\text{MoO}_3/\text{Al}_2\text{O}_3$, 5% $\text{WO}_3/\text{Al}_2\text{O}_3$, 5% $\text{CoO}/\text{Al}_2\text{O}_3$ and 6% $\text{NiO}/\text{Al}_2\text{O}_3$ samples were prepared by (incipient wetness) impregnation of an aqueous solution of ammonium heptamolybdate, ammonium metatungstate, cobalt nitrate and nickel nitrate, respectively. After the impregnation step, the samples were dried at room temperature and at 120 °C, and finally calcined in dry air at 500 °C overnight. The 5% $\text{V}_2\text{O}_5/\text{Al}_2\text{O}_3$ sample was prepared by (incipient wetness) impregnation with a solution of $\text{VO}(\text{OPr})_3$ (Alpha, 95–98% purity) in methanol. Owing to the air- and moisture-sensitive nature of this alkoxide precursor, the impregnation, subsequent drying at room temperature and heating at 350 °C were performed under a nitrogen atmosphere. The sample was finally calcined in dry air at 500 °C overnight. The mixed $\text{MO}_x\text{-V}_2\text{O}_5/\text{Al}_2\text{O}_3$ samples were prepared from $\text{MO}_x/\text{Al}_2\text{O}_3$ samples (with $\text{MO}_x = \text{MoO}_3, \text{WO}_3, \text{CoO}$ and NiO) by adding vanadium oxide as described above.

Raman studies

Raman spectra were recorded from stationary samples pressed into self-supporting wafers of *ca.* 150 mg, which were mounted into a modified version of a Raman *in situ* cell developed by

Wang and Hall.³⁶ In a typical experiment, the wafer was heated to 500 °C in *ca.* 1 h, and maintained for 1 h while ultra-high purity, hydrocarbon-free oxygen (Linde gas) was purged through the cell. The sample was then cooled to *ca.* 50 °C in *ca.* 45 min. At this temperature, the Raman spectrum was recorded on a Triplemate spectrometer (Spex, Model 1877) coupled to an optical multichannel analyser (Princeton Applied Research, Model 1463) equipped with an intensified photodiode array detector (1024 pixels, cooled to -35 °C, resolution 2 cm⁻¹). The acquisition time per scan was 30 s and 25 scans were averaged. The 514.5 nm line of an Argon ion laser (Spectra Physics) was used as the excitation source. The laser power power at the sample was 15–40 mW. None of the Raman spectra were smoothed.

FTIR studies

FTIR spectra were recorded on a Biorad FTS-7 spectrometer (resolution 2 cm⁻¹, accuracy in peak position *ca.* 2 cm⁻¹). The samples were pressed into self-supporting wafers, and mounted into a modified version of an *in situ* IR cell developed by Xiaoding.³⁷ The experimental conditions were exactly the same as those used for the Raman experiments. For monitoring the surface hydroxy group stretching region (4000–3000 cm⁻¹) self-supporting wafers of 8 mg (*ca.* 10 mg cm⁻²) were used, and 1000 scans were averaged. The spectra were smoothed to improve the signal-to-noise ratio. For recording the metal–oxygen stretching region (1100–800 cm⁻¹) and metal–oxygen first-overtone region (2150–1850 cm⁻¹), the samples were pressed into self-supporting wafers of *ca.* 5 mg (*ca.* 6 mg cm⁻²) and 20 mg (*ca.* 25 mg cm⁻²), respectively. These spectra were baseline corrected to eliminate the sloping background by subtracting the IR spectra of the alumina support. Typically 100 scans were averaged for recording the 1100–800 and 2150–1850 cm⁻¹ regions.

Results and Discussion

The catalysts used in this study are listed in Table 1. The (number of metal atoms) nm⁻² were calculated assuming a surface area of 180 m² g⁻¹ for the alumina support.

WO₃-V₂O₅/Al₂O₃ and MoO₃-V₂O₅/Al₂O₃

Metal oxide structures. The surface structures of these samples were investigated by Raman and IR spectroscopy under dehydrated conditions. The first series include the single metal oxide systems (5% V₂O₅/Al₂O₃, 5% WO₃/Al₂O₃, and 10% MoO₃/Al₂O₃), in addition to the mixed metal oxide systems (5% WO₃-5% V₂O₅/Al₂O₃ and 10% MoO₃-5% V₂O₅/Al₂O₃), and their Raman spectra are presented in Fig. 1. The Raman spectra in Fig. 1 are different from the Raman spectra of the same samples obtained under ambient conditions, which suggests that no compound formation takes place between vanadium and these additive oxides (W and Mo). The

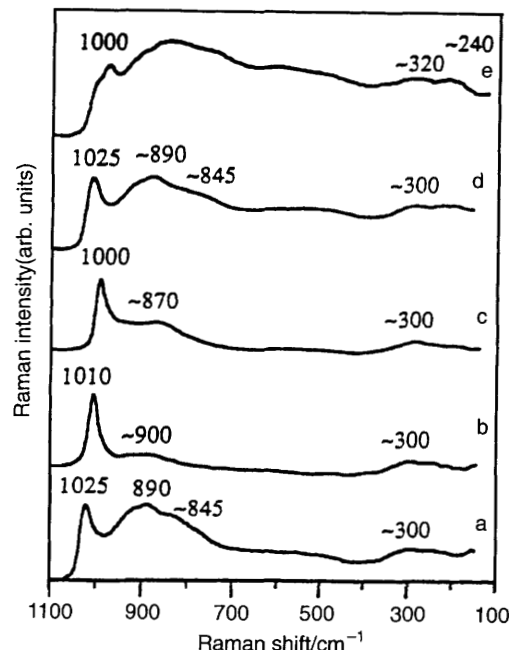


Fig. 1 Raman spectra of (a) 5% V₂O₅/Al₂O₃, (b) 5% WO₃/Al₂O₃, (c) 10% MoO₃/Al₂O₃, (d) 5% WO₃-5% V₂O₅/Al₂O₃ and (e) 10% MoO₃-5% V₂O₅/Al₂O₃ under dehydrated conditions

IR spectra of the same series of catalysts under dehydrated conditions are shown in Fig. 2 and 3 for the M=O stretching region (1100–980 cm⁻¹) and first M=O overtone region (2150–1850 cm⁻¹), respectively. IR bands of surface metal oxide species below 980 cm⁻¹ could not be detected, since they were obscured by strong absorption of the alumina support. The Raman spectrum of the 5% V₂O₅/Al₂O₃ sample [Fig. 1(a)] exhibits a narrow peak at 1025 cm⁻¹, a broad band at 890 cm⁻¹ together with a shoulder at *ca.* 845 cm⁻¹ and a weak bending mode at *ca.* 300 cm⁻¹. The 1025 cm⁻¹ band has been assigned to a V=O stretching mode of a vanadyl species, possessing one short terminal V=O bond and three bridging V–O–Al bonds.^{8,9,14–20} The IR spec-

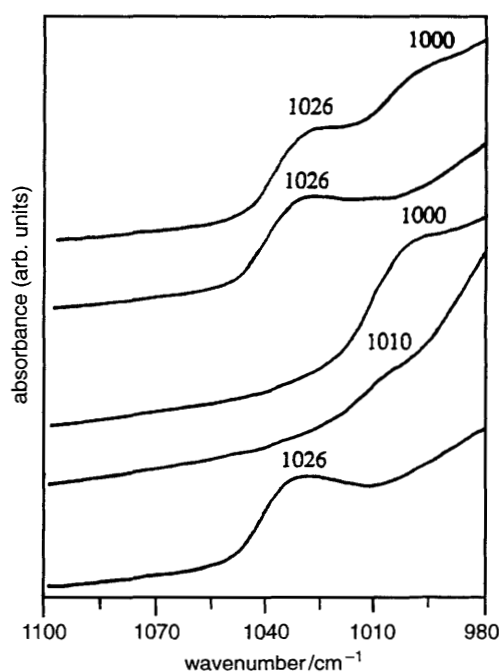


Fig. 2 IR spectra of the M=O stretching region under dehydrated conditions: (a)–(e) as Fig. 1

Table 1 Catalysts studied

catalyst	M ^a loading/ atoms nm ⁻²	V loading/ atoms nm ⁻²
5% V ₂ O ₅ /Al ₂ O ₃	—	1.84
5% WO ₃ /Al ₂ O ₃	0.72	—
10% MoO ₃ /Al ₂ O ₃	2.32	—
5% WO ₃ -5% V ₂ O ₅ /Al ₂ O ₃	0.72	1.84
10% MoO ₃ -5% V ₂ O ₅ /Al ₂ O ₃	2.32	1.84
6% NiO/Al ₂ O ₃	2.69	—
5% CoO/Al ₂ O ₃	2.23	—
6% NiO-5% V ₂ O ₅ /Al ₂ O ₃	2.69	1.84
5% CoO-5% V ₂ O ₅ /Al ₂ O ₃	2.23	1.84

^a M = W, Mo, Ni, Co.

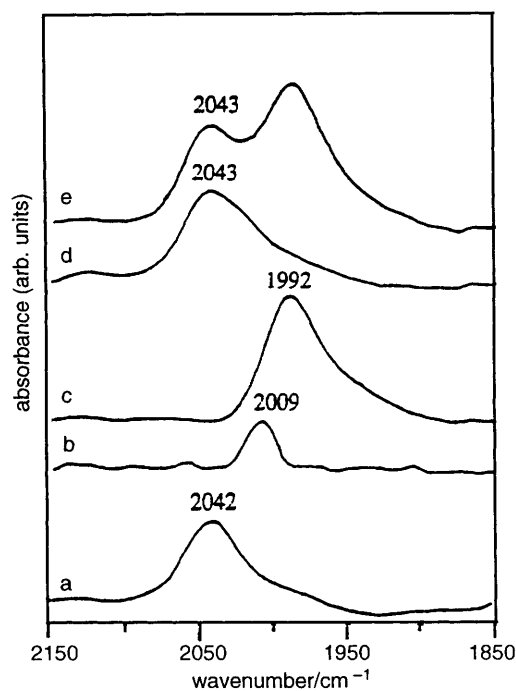


Fig. 3 IR spectra of the M=O overtone region under dehydrated conditions: (a)–(e) as Fig. 1

trum shows a band at 1026 cm^{-1} [Fig. 2(a)] and, although a similar IR band has been observed by Busca,³⁸ this is the first investigation in which both Raman and IR spectra are reported for the same $\text{V}_2\text{O}_5/\text{Al}_2\text{O}_3$ sample. The coincidence of both Raman and IR bands further supports the assignment of the 1025 cm^{-1} band to a mono-oxo vanadyl species. A vanadate species with two short V=O bonds would instead show a symmetric and antisymmetric stretching mode with the former more intense in the Raman spectrum than in the IR, and *vice versa*. Similarly, the presence of only one IR band in the overtone region at 2042 cm^{-1} [Fig. 3(a)] is also consistent with one short V=O bond. The broad Raman band at 890 cm^{-1} together with the shoulder at *ca.* 845 cm^{-1} have been attributed to polymeric vanadate species.^{15,16,19,20} This assignment is based on the similarity in position of the bands in this region with those for terminal V=O bonds of polyvanadate anions in solution or *e.g.* crystalline $\text{Zn}_2\text{V}_2\text{O}_7$.³⁹ In previous studies, it was shown that the ratio mono-oxo : polymeric vanadium oxide species decreases, and that the polymer chain becomes longer with increasing surface coverage.^{15,16,20}

The Raman spectrum of the 5% $\text{WO}_3/\text{Al}_2\text{O}_3$ sample [Fig. 1(b)] exhibits a sharp band at 1010 cm^{-1} , a weak broad band at *ca.* 900 cm^{-1} and a weak band at *ca.* 300 cm^{-1} . The 1010 cm^{-1} band has been assigned to the W=O stretching mode of a highly distorted mono-oxo (one short W=O bond) tungstate species with an octahedral coordination of the W^{6+} cation.²⁰ *In situ* X-ray absorption near-edge spectroscopy also indicated a highly distorted octahedral coordination of the W^{6+} cation.⁴⁰ The W=O stretching mode is also observed in the IR as a very weak band at *ca.* 1010 cm^{-1} [Fig. 2(b)], and its overtone occurs at *ca.* 2009 cm^{-1} [Fig. 3(b)]. The coincidence of the Raman and IR band and the presence of one band in the overtone region again support the mono-oxo model, as discussed for the vanadyl species. Both IR bands, however, appear to be very weak compared with those associated with the V=O stretching mode of the surface vanadyl [Fig. 2(a) and 3(a)]. Although the number of vanadium atoms is more than twice as that of tungsten (see Table 1), the very weak IR bands indicate that the molar absorption coefficient of mono-oxo tungsten oxide is less than of the mono-oxo

vanadium oxide. The origin of the very weak *ca.* 900 cm^{-1} Raman band is not yet clear.²⁰ It has been attributed to a small amount of microcrystalline tungstate formed from cationic impurities on the alumina surface,⁴¹ or to the W—O—W stretching mode.⁴² The latter assignment implies that the highly distorted mono-oxo tungstate is not isolated. In a previous study, additional Raman bands at *ca.* 940 , 590 and 215 cm^{-1} were observed at higher tungsten oxide loadings ($>10\%$ $\text{WO}_3/\text{Al}_2\text{O}_3$), which were attributed to polymeric tungsten oxide on the dehydrated alumina surface.²⁰

The 10% $\text{MoO}_3/\text{Al}_2\text{O}_3$ sample reveals a sharp Raman band at 1000 cm^{-1} , a broad band at *ca.* 870 cm^{-1} and a band at *ca.* 300 cm^{-1} [Fig. 1(c)]. The 1000 cm^{-1} band has been assigned to a highly distorted mono-oxo (one short Mo=O bond) molybdate species with an octahedral coordination of the Mo^{6+} cation.²⁰ The IR spectra of this sample show a band at 1000 cm^{-1} , together with its overtone at 1992 cm^{-1} [Fig. 2(c) and 3(c), respectively], which support the mono-oxo model. The origin of the very weak *ca.* 870 cm^{-1} Raman band is not yet clear.²⁰ It has been attributed to a small amount of microcrystalline molybdate formed from cationic impurities on the alumina surface.⁴³ It has, however, been proposed by other authors that the broad 870 cm^{-1} band should be assigned to the stretching mode of Mo—O—Mo linkages^{6,8} and that the presence of this band indicates the polymerized character of the mono-oxo molybdate species. In a previous study, additional Raman bands at *ca.* 940 , 580 , 360 and 208 cm^{-1} were observed at higher loadings ($>10\%$ $\text{MoO}_3/\text{Al}_2\text{O}_3$), which were attributed to polymolybdate species on the dehydrated alumina surface.²⁰

The Raman spectrum of the mixed 5% WO_3 –5% $\text{V}_2\text{O}_5/\text{Al}_2\text{O}_3$ sample [Fig. 1(d)] exhibits basically the same bands as the 5% $\text{V}_2\text{O}_5/\text{Al}_2\text{O}_3$ sample [Fig. 1(a)], although the broad 890 cm^{-1} band of the polymeric vanadium oxide surface species seems to be slightly enhanced compared with the 1025 cm^{-1} band. The Raman bands of the surface tungsten oxide species are overshadowed by the vanadium oxide bands due to the lower intensities of tungsten oxide, as discussed above. Similar observations have recently been made for the WO_3 – $\text{V}_2\text{O}_5/\text{TiO}_2$ system, which also revealed a slight increase in the concentration of polymeric vanadium oxide species.⁴⁴ The IR spectra of the M=O stretching and M=O overtone region [Fig. 2(d) and 3(d), respectively] are consistent with the Raman spectrum and reveal the V=O stretching mode of the mono-oxo vanadate species at 1026 cm^{-1} together with its overtone at 2043 cm^{-1} . Both IR bands show a weak shoulder on the low frequency side, which is due to the very weak tungsten oxide bands at *ca.* 1010 and 2010 cm^{-1} , respectively.

In the Raman spectrum of the 10% MoO_3 –5% $\text{V}_2\text{O}_5/\text{Al}_2\text{O}_3$ sample [Fig. 1(e)], the sharp band of the mono-oxo vanadium oxide species (*ca.* 1025 cm^{-1}) is now present as a shoulder on the 1000 cm^{-1} band of the mono-oxo molybdenum oxide species. The corresponding IR spectra [Fig. 2(e) and 3(e)] of this mixed oxide sample are consistent with the Raman spectrum, and show bands (overtone bands in parentheses) at 1026 (2043) cm^{-1} and *ca.* 1000 (1990) cm^{-1} of the mono-oxo vanadium and molybdenum oxide, respectively. The broad Raman band in the 800 – 900 cm^{-1} region has become broader and increased in intensity. This increase appears to be larger than the cumulative contributions of the broad bands observed in the Raman spectra of the individual systems. Furthermore, the weak bending mode shifts from *ca.* 300 to *ca.* 320 cm^{-1} and a new weak band at 240 cm^{-1} appears. These effects, the increase of the broad 800 – 900 cm^{-1} band, the shift of the bending mode and the appearance of a new band in the 200 – 250 cm^{-1} region (indicative of M—O—M bonds,²⁰) have also been observed in the single $\text{V}_2\text{O}_5/\text{Al}_2\text{O}_3$ and $\text{MoO}_3/\text{Al}_2\text{O}_3$ systems with increasing coverage, and indicate the formation of more polymerized surface-metal-oxide

species.²⁰ Thus, the presence of both molybdenum oxide (or tungsten oxide) and vanadium oxide on the dehydrated surface has the same effect on the metal oxide structures as increasing the surface coverage of the corresponding single component systems.

Support hydroxy groups. The OH stretching region of the Al_2O_3 support, and of the first series of samples are shown in Fig. 4. Pure alumina exhibits three major IR bands at 3775, 3730 and 3680 cm^{-1} , which have been assigned to basic, neutral and acidic OH groups, respectively.³ Upon addition of 5% V_2O_5 , 5% WO_3 or 10% MoO_3 [Fig. 4(a), (b) and (c), respectively], the intensities of these hydroxy group stretching modes, especially those of the basic and neutral hydroxy groups, decrease. The consumption of hydroxy groups is less pronounced in the IR spectrum of the 5% $\text{WO}_3/\text{Al}_2\text{O}_3$ sample [Fig. 4(b)] owing to the metal oxide loading of this sample being lower than the vanadium and molybdenum oxide samples (see Table 1). The consumption is very clear in the case of 10% $\text{MoO}_3/\text{Al}_2\text{O}_3$ [Fig. 4(c)], in which most of the basic hydroxy groups (3775 cm^{-1} band), and a large part of the neutral hydroxy groups (3730 cm^{-1} band) and acidic hydroxy groups (3680 cm^{-1} band) are removed. These findings are in agreement with other IR studies and show that metal oxides with a high oxidation state such as vanadium, tungsten and molybdenum oxide consume the same type of hydroxy groups.²¹

The IR spectrum of the mixed 5% WO_3 -5% $\text{V}_2\text{O}_5/\text{Al}_2\text{O}_3$ sample [Fig. 4(d)] reveals a further reduction compared with the single 5% $\text{WO}_3/\text{Al}_2\text{O}_3$ and 5% $\text{V}_2\text{O}_5/\text{Al}_2\text{O}_3$ systems. The depletion of OH_{Al} groups is very extensive in the case of 10% MoO_3 -5% $\text{V}_2\text{O}_5/\text{Al}_2\text{O}_3$, and only a weak, broad band remains in the IR spectrum [Fig. 4(e)]. Similar observations have been made in previous IR studies on the single $\text{V}_2\text{O}_5/\text{Al}_2\text{O}_3$, $\text{WO}_3/\text{Al}_2\text{O}_3$ and $\text{MoO}_3/\text{Al}_2\text{O}_3$ systems with increasing metal oxide loadings.²¹ Thus, the addition of two metal oxides, which have high oxidation states, to the alumina support results in competition for the same alumina hydroxy groups, and has the same effect as increasing the surface coverage in the single component systems. The IR spectra showing the OH stretching region, however, do not reveal any

information on the possible interaction of metal oxide species with other alumina surface sites such as Lewis acid sites (coordinative unsaturated sites), as will be discussed below.

$\text{NiO-V}_2\text{O}_5/\text{Al}_2\text{O}_3$ and $\text{CoO-V}_2\text{O}_5/\text{Al}_2\text{O}_3$

Metal oxide structures. The Raman spectra of the second series of catalysts, which includes the single 6% $\text{NiO}/\text{Al}_2\text{O}_3$ and 5% $\text{CoO}/\text{Al}_2\text{O}_3$ systems and the mixed 6% NiO -5% $\text{V}_2\text{O}_5/\text{Al}_2\text{O}_3$ and 5% CoO -5% $\text{V}_2\text{O}_5/\text{Al}_2\text{O}_3$ samples, are presented in Fig. 5. The Raman spectrum of the 5% $\text{V}_2\text{O}_5/\text{Al}_2\text{O}_3$ sample is also included for comparison. The Raman spectra in Fig. 5 are different from the Raman spectra of the same samples obtained under ambient conditions, which suggests that no compound formation takes place between vanadium and these additive oxides (Ni and Co). The Raman spectrum of the 6% $\text{NiO}/\text{Al}_2\text{O}_3$ catalyst reveals a broad band at 550 cm^{-1} [Fig. 5(b)], which has been assigned to a surface nickel(II) oxide phase with the nickel incorporated into the subsurface of the alumina support.¹ Support for this assignment can be found in a variety of spectroscopic studies, *e.g.* X-ray photoelectron spectroscopy, ion scattering spectroscopy, diffuse reflectance spectroscopy, extended X-ray absorption fine structure spectroscopy and photoacoustic spectroscopy.²⁴⁻²⁷ These studies revealed that nickel oxide diffuses into the surface octahedral and tetrahedral sites of γ -alumina to form stoichiometric or non-stoichiometric surface spinel compounds. The ratio of octahedrally coordinated nickel to tetrahedrally coordinated nickel ($\text{Ni}_{\text{oct}}:\text{Ni}_{\text{tet}}$) was found to be dependent on the calcination temperature. A diffuse reflectance spectroscopy study by Scheffer *et al.* showed that these octahedrally coordinated Ni^{2+} ions experience a weaker field than NiAl_2O_4 and it was argued that the Ni_{oct} are located near the surface, while the Ni_{tet} ions are located in the bulk of the alumina support.²⁴

The Raman spectrum of the single 5% $\text{CoO}/\text{Al}_2\text{O}_3$ sample [Fig. 5(c)] exhibits weak bands at *ca.* 680, 600 and 475 cm^{-1} . The *ca.* 680 and *ca.* 475 cm^{-1} bands match those of crystalline Co_3O_4 particles, although they are slightly shifted to lower wavenumber and somewhat broader, indicating a small par-

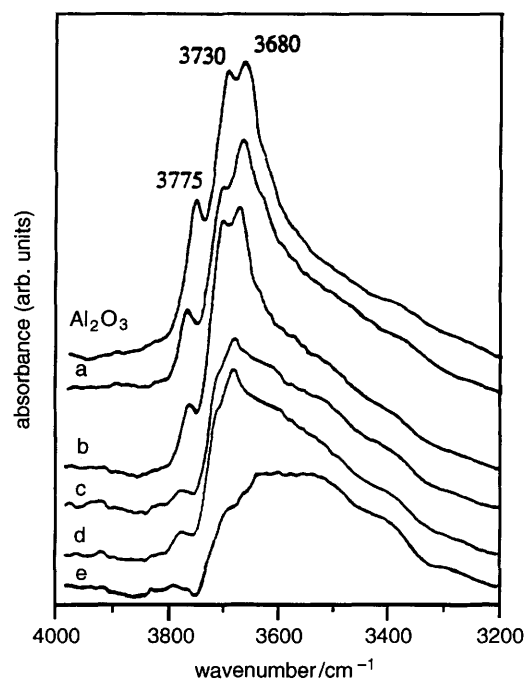


Fig. 4 IR spectra of the hydroxy group region under dehydrated conditions: (a)–(e) as Fig. 1. The spectrum of the alumina support is also shown.

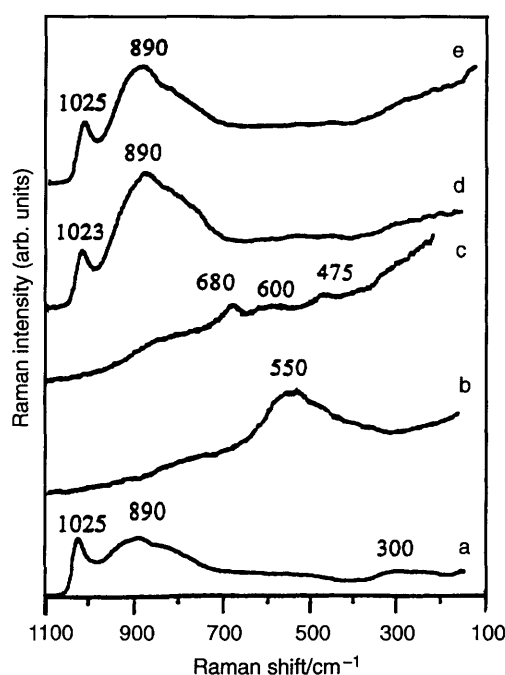


Fig. 5 Raman spectra of (a) 5% $\text{V}_2\text{O}_5/\text{Al}_2\text{O}_3$, (b) 6% $\text{NiO}/\text{Al}_2\text{O}_3$, (c) 5% $\text{CoO}/\text{Al}_2\text{O}_3$, (d) 6% NiO -5% $\text{V}_2\text{O}_5/\text{Al}_2\text{O}_3$ and (e) 5% CoO -5% $\text{V}_2\text{O}_5/\text{Al}_2\text{O}_3$ under dehydrated conditions

tle character.³⁰ The broad *ca.* 600 cm^{-1} band has been assigned to a dispersed surface cobalt oxide phase.³⁰ Other studies also concluded that in $\text{CoO}/\text{Al}_2\text{O}_3$ a dispersed phase is present, which consists of Co^{2+} ions in the surface layers of the alumina support.^{28–33} It was demonstrated that these Co^{2+} ions are non-reducible and non-sulfidable, which suggests that they are located in the surface of the alumina support.^{31,32} Mössbauer spectroscopy and IR chemisorption studies, however, showed that some of the cobalt ions are octahedrally coordinated.^{29,35} These cobalt ions were not identified earlier by diffuse reflectance spectroscopy, since this technique is not very sensitive to Co in octahedral coordination. The Co_{oct} ions were shown to be affected by sulfiding treatment and accessible for NO adsorption, which suggests that these cobalt ions are located near the alumina surface.^{28,41}

The Raman spectra of the mixed 6% NiO–5% $\text{V}_2\text{O}_5/\text{Al}_2\text{O}_3$ [Fig. 5(d)] and 5% CoO–5% $\text{V}_2\text{O}_5/\text{Al}_2\text{O}_3$ samples [Fig. 5(e)] show the V=O stretching mode of the mono-oxo vanadium oxide at 1023 and 1025 cm^{-1} , respectively. This is in agreement with the IR spectra, which reveal this band at 1024 and 1025 cm^{-1} [Fig. 6(b) and 6(c)] and the first V=O overtone at 2039 and 2041 cm^{-1} [Fig. 7(b) and 7(c)], respectively. The weak Raman bands of the supported nickel and cobalt oxides are overshadowed by the bands of the supported vanadium oxide species, because the Raman intensities of the nickel and cobalt oxide phases are smaller. A low Raman intensity is commonly found for metal oxides with low valency, since they possess forbidden ligand-field transitions in the visible region, causing a decrease in Raman intensity.²⁵ Thus, the Raman spectra do not provide information on the influence of the surface vanadium oxide species on the nickel and cobalt oxide phases. The Raman spectra of the mixed oxide samples, however, show that in the presence of nickel or cobalt oxide the 890 cm^{-1} band becomes much more intense [Fig. 5(d) and 5(e)]. Thus, the combined Raman and IR spectra show that the mono-oxo and polymeric vanadium oxide structures are not changed by the presence of nickel or cobalt oxide, since the 1015 and 890 cm^{-1} bands are hardly shifted in frequency. The enhanced intensity of the 890 cm^{-1} band, however, indicates that the presence of nickel or cobalt oxide promotes the

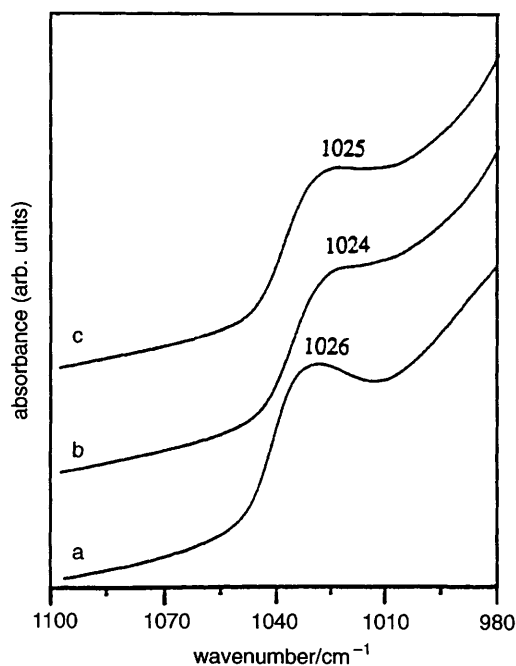


Fig. 6 IR spectra of M=O stretching region under dehydrated conditions of (a) 5% $\text{V}_2\text{O}_5/\text{Al}_2\text{O}_3$, (b) 6% NiO–5% $\text{V}_2\text{O}_5/\text{Al}_2\text{O}_3$ and (c) 5% CoO–5% $\text{V}_2\text{O}_5/\text{Al}_2\text{O}_3$

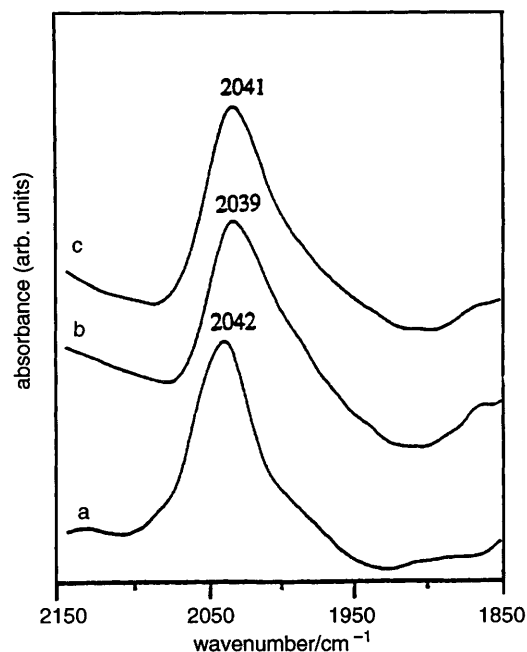


Fig. 7 IR spectra of the first overtone M=O stretching region under dehydrated conditions: (a)–(c) as Fig. 6

formation of the polymeric vanadium oxide species under dehydrated conditions. The enhancement of the 800–900 cm^{-1} band is much greater than observed for the $\text{MoO}_3\text{--V}_2\text{O}_5/\text{Al}_2\text{O}_3$ sample [Fig. 1(e)], and demonstrates that the presence of cobalt or nickel oxide influences the supported vanadium oxide phase much more than the presence of molybdenum oxide or tungsten oxide. The enormous impact of nickel and cobalt oxide on the vanadium oxide species also indicates that (part of) the nickel and cobalt oxide must be located in the surface region near the vanadium oxide species.

Support hydroxy groups. The interaction of the metal oxides of the second series with the alumina hydroxy groups is shown in Fig. 8. The IR spectra of Al_2O_3 and 5% $\text{V}_2\text{O}_5/\text{Al}_2\text{O}_3$ [Fig. 8(a)] are again shown for comparison. Addition of 6% NiO to the alumina results in a slight intensity decrease of the 3775 and 3680 cm^{-1} bands of the basic and acidic hydroxy groups, respectively, but does not influence the neutral hydroxy groups [Fig. 8(b)]. The 5% CoO/ Al_2O_3 sample reveals a slight decrease of only the basic hydroxy group band at 3775 cm^{-1} [Fig. 8(c)]. Although the IR spectra reveal that nickel and cobalt oxide react to some extent with the alumina hydroxy groups, it is clearly not as extensive as for vanadium and molybdenum oxide. The 6% NiO–5% $\text{V}_2\text{O}_5/\text{Al}_2\text{O}_3$, and 5% CoO–5% $\text{V}_2\text{O}_5/\text{Al}_2\text{O}_3$ samples show basically the same IR spectra, with a further reduction of the basic hydroxy group band (3775 cm^{-1}) as the 5% $\text{V}_2\text{O}_5/\text{Al}_2\text{O}_3$ sample, as shown in Fig 8(d) and 8(e), respectively.

Based on a simple correlation between the metal oxide surface structures and the depletion of specific hydroxy groups of the support, a huge increase in concentration of polymeric vanadium oxide species should coincide with a dramatic decrease of neutral and acidic alumina hydroxy groups. However, this is not observed in the IR spectra of the mixed 5% CoO–5% $\text{V}_2\text{O}_5/\text{Al}_2\text{O}_3$ and 6% NiO–5% $\text{V}_2\text{O}_5/\text{Al}_2\text{O}_3$ samples [Fig. 8(d) and 8(e)]. Moreover, the IR spectra of the 5% $\text{WO}_3\text{--V}_2\text{O}_5/\text{Al}_2\text{O}_3$ and the 6% NiO–5% $\text{V}_2\text{O}_5/\text{Al}_2\text{O}_3$ are similar [Fig. 4(d) and 8(d), respectively], but the ratios of mono-oxo : polymeric vanadium oxide are completely different [Fig. 1(c) and 5(d), respectively]. Thus, the correlation between the surface metal oxide structures of *e.g.* vanadium,

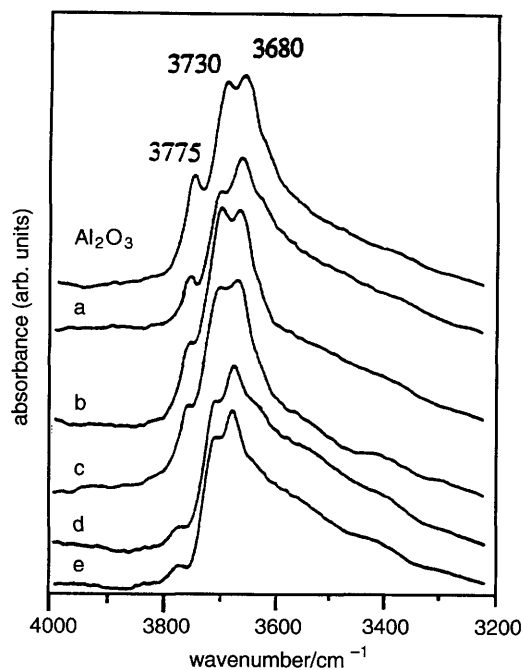


Fig. 8 IR spectra of the hydroxy group region under dehydrated conditions: (a)–(f) as Fig. 5. The spectrum of the alumina support is also shown.

molybdenum and tungsten oxide, and the depletion of specific alumina hydroxy groups is less straightforward than expected on the basis of structural changes of these metal oxide species and consumption of hydroxy groups with increasing loading.^{20,21}

A possible explanation could be that metal oxide species do not only interact with the surface by reaction with hydroxy groups, but also interact with other surface sites on alumina such as Lewis acid (coordinative unsaturated Al^{3+}) centres (approximately one out of seven alumina sites, depending on the calcination temperature⁴⁵). These interactions will not be observed in the 4000–3000 cm^{-1} region of the IR spectra, since they do not involve hydroxy groups. Infrared pyridine chemisorption can be used to identify Lewis acid sites (presence and acid strength), but the results reported in the literature have not been straightforward. The reason is that the addition of a metal oxide might consume Lewis acid sites, but can also generate new Lewis acid centres.^{46–48} The number of Lewis acid sites has been reported to increase with increasing loading, e.g. the $\text{WO}_3/\text{Al}_2\text{O}_3$ system,⁴⁷ but to decrease upon addition of molybdenum or vanadium oxide to alumina.²¹ The influence on the Lewis acid sites upon addition of cobalt or nickel oxide has not been reported in the literature, but preliminary pyridine adsorption experiments in our laboratory show that the cobalt and nickel oxide slightly decrease the number of alumina Lewis acid sites.⁴⁹ Experiments by Van Veen and co-workers on the $\text{MoO}_3/\text{Al}_2\text{O}_3$ system have indicated that at low loading the molybdenum oxide reacts with the basic hydroxy groups, while at higher loadings molybdenum oxide is physisorbed on the Lewis acid sites.^{50–52} Although the decrease of neutral and acidic hydroxy groups at high molybdenum oxide loading cannot be satisfactorily explained by this model, it supports the possibility that not only the surface hydroxy groups are involved in the interaction between metal oxide species and support surface, but also support Lewis acid sites. A competition between cobalt or nickel oxide (sub)surface species and vanadium oxide species for reaction with these Lewis acid sites would account for the crowding caused by nickel and cobalt oxide. This crowding is experienced by the vanadium oxide species as an increase in surface coverage leading to an increase of

concentration of polymeric vanadium oxide species. Thus, the Raman spectra clearly show that cobalt and nickel oxide strongly influence the surface vanadium oxide species but more work is required to understand the exact nature of this interaction.

Conclusions

The influence of a second metal oxide (tungsten oxide, molybdenum oxide, nickel oxide or cobalt oxide) on a $\text{V}_2\text{O}_5/\text{Al}_2\text{O}_3$ catalyst has been investigated by a combined Raman and IR study under dehydrated conditions. The presence of tungsten or molybdenum oxide was found to increase the concentration of polymerized surface vanadium oxide species, and this reflects the higher surface coverages of the oxides on the alumina support. This is probably caused by competition between vanadium and molybdenum oxide (or vanadium and tungsten oxide) species for reaction with the alumina hydroxy groups, since the IR spectra reveal that upon addition of these metal oxides, the same type of alumina hydroxy groups are consumed. The presence of nickel or cobalt oxide on alumina increases the concentration of polymerized vanadium oxide species dramatically, which indicates that the presence of these oxides is also experienced by the vanadium oxide as an increase in surface coverage. The mechanism for the influence of cobalt or nickel oxide on the surface vanadium oxide species, however, is not clear since the alumina hydroxy groups are not extensively consumed by cobalt or nickel oxide.

The authors would like to thank Professor Dr. W. K. Hall and Dr. J. C. Mol for providing the *in situ* Raman and IR cells, respectively. G.D. and I.E.W. would like to acknowledge the financial support of the Department of Energy, Basic Science Division (Grant #DE-FG02-93ER 14350).

References

- 1 S. S. Chan and I. E. Wachs, *J. Catal.*, 1987, **103**, 224.
- 2 G. Deo and I. E. Wachs, *J. Phys. Chem.*, 1991, **95**, 5889.
- 3 H.-P. Boehm and H. Knözinger, *Catalysis*, ed. J. R. Anderson and M. Boudart, Springer-Verlag, Berlin, 1983, vol. 4, p. 39.
- 4 M. A. Vuurman, I. E. Wachs, D. J. Stufkens and A. Oskam, *J. Mol. Catal.*, 1992, **77**, 263.
- 5 J. M. Stencel, L. E. Makovsky, T. A. Sarkus, J. De Vries, R. Thomas and J. A. Moulijn, *J. Catal.*, 1984, **90**, 314.
- 6 J. M. Stencel, L. E. Makovsky, J. R. Diehl and T. A. Sarkus, *J. Catal.*, 1985, **95**, 414.
- 7 J. M. Stencel, L. E. Makovsky, J. R. Diehl and T. A. Sarkus, *J. Raman Spectrosc.*, 1984, **15**, 282.
- 8 E. Payen, S. Kasztelan, J. Grimblot and J. P. Bonnell, *J. Raman Spectrosc.*, 1986, **17**, 233.
- 9 E. Payen, S. Kasztelan, J. Grimblot and J. P. Bonnell, *J. Mol. Struct.*, 1986, **143**, 259.
- 10 S. S. Chan, I. E. Wachs, L. L. Murrell, L. Wang and W. K. Hall, *J. Phys. Chem.*, 1984, **88**, 5831.
- 11 M. A. Vuurman, I. E. Wachs, D. J. Stufkens and A. Oskam, *J. Mol. Catal.*, 1993, **80**, 209.
- 12 J. M. Jehng and I. E. Wachs, *Catal Today*, 1990, **8**, 37.
- 13 J. M. Jehng and I. E. Wachs, *J. Phys. Chem.*, 1991, **95**, 7373.
- 14 L. R. Le Coustumer, B. Taouk, M. Le Meur, E. Payen, M. Guelton and J. Grimblot, *J. Phys. Chem.*, 1988, **92**, 1230.
- 15 S. T. Oyama, G. Went, K. B. Lewis, A. T. Bell and G. Somarjai, *J. Phys. Chem.*, 1989, **93**, 6786.
- 16 G. T. Went, S. T. Oyama and A. T. Bell, *J. Phys. Chem.*, 1990, **94**, 4240.
- 17 G. Deo, H. Eckert and I. E. Wachs, *Prep. Am. Chem. Soc. Div. Petrol. Chem.*, 1990, **35**, 16.
- 18 I. E. Wachs, *Chem. Eng. Sci.*, 1990, **45**, 2561.
- 19 I. E. Wachs, *J. Catal.*, 1991, **129**, 307.
- 20 M. A. Vuurman and I. E. Wachs, *J. Phys. Chem.*, 1992, **96**, 5008.
- 21 A. M. Turek, I. E. Wachs and E. DeCanio, *J. Phys. Chem.*, 1992, **96**, 5000.
- 22 M. Sibeijn, R. Spronk, J. A. R. van Veen and J. C. Mol, *Cat. Lett.*, 1991, **8**, 2.

- 23 K. Segawa and W. K. Hall, *J. Catal.*, 1982, **76**, 133.
24 L. Zhang, J. Lin and Y. Chen, *J. Chem. Soc., Faraday Trans.*, 1992, **88**, 497.
25 B. Scheffer, J. J. Heijeinga and J. A. Moulijn, *J. Phys. Chem.*, 1987, **91**, 4752.
26 M. Wu and D. M. Hercules, *J. Phys. Chem.*, 1979, **83**, 2003.
27 L. W. Burggraf, D. E. Leyden, R. L. Chin and D. M. Hercules, *J. Catal.*, 1982, **78**, 360.
28 P. Arnoldy and J. A. Moulijn, *J. Catal.*, 1985, **93**, 38.
29 C. Wivel, B. S. Clausen, R. Candia, S. Mørup and H. Topsøe, *J. Catal.*, 1984, **87**, 497.
30 M. Kellner and I. E. Wachs, to be published.
31 M. Lo Jacono, V. L. Verbeek and G. C. A. Schuit, *J. Catal.*, 1973, **29**, 463.
32 R. I. Declerck-Grimee, P. Canesson, R. M. Friedman and J. J. Fripiat, *J. Phys. Chem.*, 1978, **83**, 885.
33 M. A. Stranick, M. Houalla and D. Hercules, *J. Catal.*, 1990, **125**, 214.
34 M. A. Vuurman and I. E. Wachs, *J. Mol. Catal.*, 1992, **77**, 29.
35 N.-Y. Topsøe and H. Topsøe, *J. Catal.*, 1982, **75**, 354.
36 L. Wang and W. K. Hall, *J. Catal.*, 1983, **82**, 177.
37 Xu Xiaoding, Ph.D. Thesis, University of Amsterdam, The Netherlands, 1985.
38 G. Busca, *Mater. Chem. Phys.*, 1988, **19**, 157.
39 W. P. Griffith and T. D. Wickins, *J. Chem. Soc. A*, 1966, 1087.
40 J. A. Horsley, I. E. Wachs, J. M. Brown, G. H. Via and F. D. Hardcastle, *J. Phys. Chem.*, 1987, **91**, 4041.
41 F. D. Hardcastle and I. E. Wachs, *J. Raman Spectrosc.*, 1995, **26**, 397.
42 J. M. Stencel, *Raman Spectroscopy for Catalysis*, van Nostrand Reinhold, New York, 1990.
43 F. D. Hardcastle and I. E. Wachs, *J. Raman Spectrosc.*, 1990, **21**, 683.
44 M. A. Vuurman, I. E. Wachs and A. M. Hirt, *J. Phys. Chem.*, 1991, **95**, 9928.
45 B. A. Morrow, in *Studies in Surface Science and Catalysis 57, Spectroscopic Characterization of Heterogeneous Catalysts, part A*, ed. J. L. G. Fierro, Elsevier, Amsterdam, 1990, p. 161.
46 J. M. Jehng, A. M. Turek and I. E. Wachs, *Appl. Catal. A*, 1992, **83**, 179.
47 R. Zhang, J. Jagiello, J. H. Hu, Z.-Q. Huang and J. A. Schwartz, *Appl. Catal. A*, 1992, **84**, 123.
48 G. Connell and J. A. Dumesic, *J. Catal.*, 1986, **102**, 216.
49 A. M. Turek and I. E. Wachs, unpublished results.
50 C. T. J. Mensch, J. A. R. van Veen, B. van Wingerden and M. P. van Dijk, *J. Phys. Chem.*, 1988, **92**, 4961.
51 J. A. R. van Veen, G. Jonkers and W. H. Hesselink, *J. Chem. Soc., Faraday Trans. 1*, 1989, **85**, 389.
52 J. A. R. van Veen, P. A. J. M. Hendriks, E. J. G. M. Romers and R. R. Andréa, *J. Phys. Chem.*, 1990, **94**, 5275.

Paper 6/01349J; Received 26th February, 1996